Hydrodynamic interaction of trapped active Janus particles in two dimensions

Tanwi Debnath,[1] Yunyun Li,[2,3,*] Pulak K. Ghosh,[4] and Fabio Marchesoni[2,5]
[1]*Department of Chemistry, University of Calcutta, Kolkata 700009, India*
[2]*Center for Phononics and Thermal Energy Science, School of Physics Science and Engineering, Tongji University, Shanghai 200092, People's Republic of China*
[3]*Shanghai Key Laboratory of Special Artificial Microstructure Materials and Technology, School of Physics Science and Engineering, Tongji University, Shanghai 200092, China*
[4]*Department of Chemistry, Presidency University, Kolkata 700073, India*
[5]*Dipartimento di Fisica, Università di Camerino, I-62032 Camerino, Italy*

(Received 3 November 2017; revised manuscript received 17 February 2018; published 9 April 2018)

The dynamics of a pair of identical artificial microswimmers bound inside two harmonic traps, in a thin sheared fluid film, is numerically investigated. In a two-dimensional Oseen approximation, the hydrodynamic pair coupling is long-ranged and proportional to the particle radius to film thickness ratio. On increasing such ratio above a certain threshold, a transition occurs between a free regime, where each swimmer orbits in its own trap with random phase, and a strong synchronization regime, where the two swimmers strongly repel each other to an average distance larger than both the trap distance and their free orbit diameter. Moreover, the swimmers tend to synchronize their positions opposite the center of the system.

DOI: 10.1103/PhysRevE.97.042602

I. INTRODUCTION

The motion of artificial microswimmers is generally associated with backflows in the suspension fluid, the properties of which greatly vary with their self-propulsion mechanism [1–4]. This immediately raises the issue of how hydrodynamics influences the diffusion of active particles at the geometric boundaries [5,6], in sheared flows [7,8], and, even more, when clustering [9,10].

We investigated the hydrodynamic interactions between two microswimmers moving in a free-standing film at low Reynolds numbers [11–13] subject to a Couette shear. The problem is important in the context of the emerging technology of synthetic active matter [14]. For instance, thinking of biomedical and environmental applications, active particles can be designed to operate inside the surface layers of organic tissues [15] or natural water surfaces. This situation should not be mistaken with the quasi-two-dimensional (2D) setups frequently reported in the literature, for instance, by spatially confining active colloids between two parallel boundaries [12,15] or letting them sediment, under the action of gravity, at the bottom of a container [16]. In all these setups, momentum flow of the suspension fluid is not restricted on a plane, so that calculating the relevant hydrodynamic effects remains an intrinsically 3D task (though with more complicated boundary conditions [5,6]).

The stochastic motion of a free particle following the streamlines of a viscous sheared fluid and the motion of the same particle trapped in a harmonic well swept through by the same shear flow, can be conveniently related [17,18]. Of course, trapped particles (e.g., in an optical tweezer) allow an easier experimental observation of sheared Brownian motion [19]. We propose to generalize this approach to investigate the hydrodynamic pair interaction of self-propelling swimmers in 2D. To this purpose we numerically simulated two identical active spheres diffusing in distinct harmonic planar traps, placed away from any other obstacle [Fig. 1(a)] to neglect unwanted hydrodynamic interactions with the flow bound-aries [20].

Hydrodynamic interactions in 2D are characterized by long-range tails of the fluid flow propagator [11]. To explicitly account for the far-field properties of the system we adopted a refined version of the 2D Oseen tensor [21] recently proposed and experimentally validated by Di Leonardo *et al.* [13] for passive colloidal particles. As the 2D Oseen tensor is proportional to the particle radius to film thickness ratio, so is the pair hydrodynamic coupling. Increasing the particles' radius at constant film thickness bears remarkable effects on the pair dynamics [see sketch in Fig. 1(b)]. Small radius particles tend to perform elliptical orbits inside the traps, subjected to the shear torque. The size of their orbits depends on their self-propulsion speed and the trap strength, whereas their phases vary randomly with time due to angular noise associated with the self-propulsion mechanism. For particle radii larger than a certain value, which depends on the distance between traps, hydrodynamics interactions make the average pair distance jump to values that exceed and only weakly depend on the trap distance. Simultaneously, the swimmers synchronize their phases to move, in average, opposite one another with respect to the midpoint between the traps.

This paper is organized as follows. In Sec. II we introduce the Langevin equations that model two harmonically trapped active JP's suspended in a thin fluid film and coupled via a 2D Oseen tensor. In Sec. III we numerically investigate their hydrodynamic interactions, first in the no-shear regime. As anticipated above, the two particles repel one another with increasing the hydrodynamic coupling constant, while

*Corresponding author: yunyunli@tongji.edu.cn

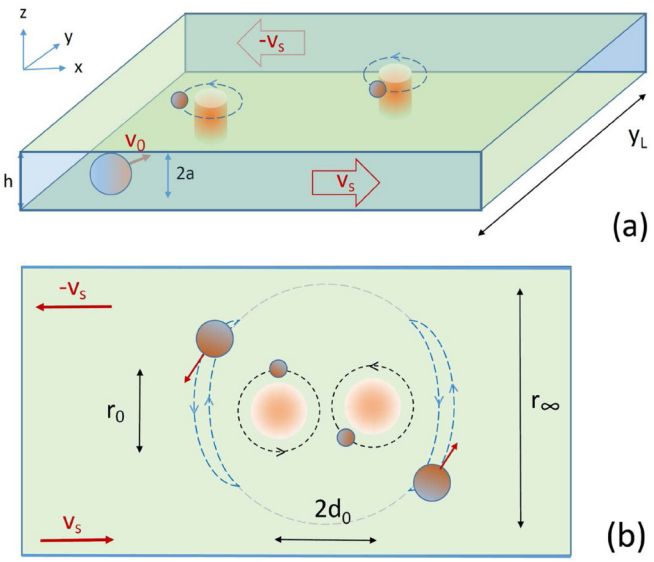

FIG. 1. Trapped active Janus particles in a thin sheared free-standing film of thickness h and width y_L: (a) Ideal experimental setup. A pair of identical Janus particles of radius a diffusing in a planar Couette cell are trapped by orthogonal optical tweezers of equal strength k (orange cylinders). v_0 and $\pm v_s$ are the speeds respectively of the self-propelling particles and the Couette cell walls. (b) Illustration of the hydrodynamic effects on the pair dynamics: small-radius particles orbit inside harmonic traps, placed a distance d_0 apart, with average radius $r_0 = v_0/k$ and random phases; large-radius particles repel one another and synchronize their phases, keeping an average distance, r_∞, much larger than d_0.

synchronizing their orbits. The additional effects of a planar shear flow of the Couette's type on the pair's dynamics is briefly discussed in Sec. IV. Finally, in Sec. V we draw some concluding remarks.

II. MODEL

The overdamped dynamics of the active pair was modeled by a set of coupled Langevin equations

$$\dot{\mathbf{R}}_i = \mathbf{F}_i + \mathbf{G}(\mathbf{R}_i - \mathbf{R}_j)\mathbf{F}_j(\mathbf{R}_j) + \mathbf{u}_i + \mathbf{v}_{0,i}, \qquad (1)$$

where, in Einstein summation convention, the subscripts i and j refer to the pair components 1 and 2, respectively, $\mathbf{R}_i = (x_i, y_i)$ denote their positions in the plane (x, y), $\mathbf{v}_{0,i}$ their self-propulsion velocity, and $\mathbf{u}_i$ is the shear flow acting upon them. For simplicity, we assumed a planar Couette flow [21,22] oriented along the x axis, $\mathbf{u}_i = -2\Omega y_i \hat{\mathbf{x}}$. The vector $\mathbf{F}_i$ is the restoring drive the ith (ideally non-truncated [23]) harmonic trap of strength k and center $\mathbf{d}_i$ exerts on the particle of coordinates $\mathbf{R}_i$, that is,

$$\mathbf{F}_i(\mathbf{R}_i) = -k(\mathbf{R}_i - \mathbf{d}_i). \qquad (2)$$

In the overdamped regime of Eq. (1) the vectors $\mathbf{F}_i$ have the dimensions of a force divided by a viscous constant (the same for both particles). In our simulations we always placed the traps symmetrically with respect to the origin, so that $\mathbf{d}_1 = -\mathbf{d}_2 = \mathbf{d}_0$. If, contrary to our assumption, the two non-truncated harmonic traps were taken to act on both active JP's, the total restoring force on the ith particle would add up to $\mathbf{F}_i = -2k\mathbf{R}_i$. The ensuing hydrodynamic pair interaction would then be still described by the present model, but with $\mathbf{d}_0 = 0$ and doubled trap strength.

For a structureless swimmer [24,25], like the active Janus particles (JP) considered here, the self-propulsion velocities, $\mathbf{v}_{0,i} = v_0(\cos\phi_i, \sin\phi_i)$, on the right-hand side (r.h.s.) of Eq. (1) have the same constant modulus, v_0, while their orientations, ϕ_i, relative to the flow direction, vary with time subjected to the orthogonal shear torques [26,27], $\Omega_i = -(1/2)\nabla \times \mathbf{u}_i$, and the stationary Gaussian noises $\xi_i(t)$ with $\langle \xi_i(t) \rangle = 0$ and $\langle \xi_i(t)\xi_j(0) \rangle = 2\delta_{ij} D_\phi \delta(t)$, that is, $\dot{\phi}_i = \Omega + \xi_i(t)$.

The dynamics of JP 1 and 2 is coupled via the 2D Oseen tensor [13,22],

$$\mathbf{G}^{\alpha\beta}(\mathbf{r}) = \frac{a}{h}\left[\delta^{\alpha\beta}\left(\ln\frac{L}{r} - 1\right) + \frac{r^\alpha r^\beta}{r^2}\right], \qquad (3)$$

where α and β denote the Cartesian projections x and y of the particles' separation vector, $\mathbf{r} = \mathbf{R}_j - \mathbf{R}_i$ with $i \neq j$. Here, a and h are the particle radius and the film thickness shown in Fig. 1(a), where $2a < h$. The cut-off length L ensures that for $r \ll L$ three main assumptions hold: (1) infinite size of the film; (2) negligible inertia; (3) negligible viscous drag at the interfaces. The last assumption, in particular, requires that the viscosity of the bounding fluid is much smaller than the viscosity of the film itself. In the present study, consistently with many practical realizations [13], L was taken considerably larger than the film thickness, h, to ensure the validity of the 2D model also in the limit $a/h \to 0$.

In the absence of a trapping force, both active JP's would move force-free despite the fact that each establishes a velocity, $\mathbf{v}_{0,i}$, which, in the overdamped regime, one may model as a self-propulsion "force" [28]. However, these are not real forces and, therefore, a free self-propelling swimmer couples hydrodynamically to other particles only through higher derivatives of the Green tensor (a higher order effect we neglect). On the contrary, the trapping forces, $\mathbf{F}_i$, do induce Stokeslets and are therefore coupled via the Oseen tensor in Eq. (1).

To single out the system's free parameters we rescaled space and time, $r_\alpha \to r'_\alpha = r_\alpha/(v_0/k)$ and $t \to t' = kt$. The remaining tunable parameters are the hydrodynamic pair coupling, a/h, the trap half-distance, $d'_0 = d_0/(v_0/k)$, and the active JP angular dynamics parameters, $\Omega' = \Omega/k$ and $D'_\phi = D_\phi/k$. In our simulations [29] we implicitly used dimensionless units by setting $k = v_0 = 1$ and dropping the prime signs altogether.

III. NO-SHEAR REGIME, Ω = 0

Contour plots for the 2D probability density functions (p.d.f.), $P_i(x, y)$, of a pair of trapped active JP's moving in a unsheared film of constant thickness, h, are displayed in Fig. 2 for two different trap distances and increasing particle radii. In the panels of the top row $\mathbf{d}_0 = 0$, that is the two swimmers move effectively inside the same trap (their collisions are ignored). In the panels of the bottom row, the traps of JP 1 and 2 were shifted vertically by $\pm y_0$ from the origin, $\mathbf{d}_0 = (0, y_0)$. A few interesting properties are apparent: (i) At low hydrodynamic coupling, the $P_i(x, y)$ contour plots exhibit a thin annular structure with radius v_0/k and centers at $(0, \pm y_0)$ [panels (a), (e)]; (ii) On increasing a, for $y_0 = 0$, the annular structures spread out radially [panel (b)], whereas, for $y_0 > 0$, the two

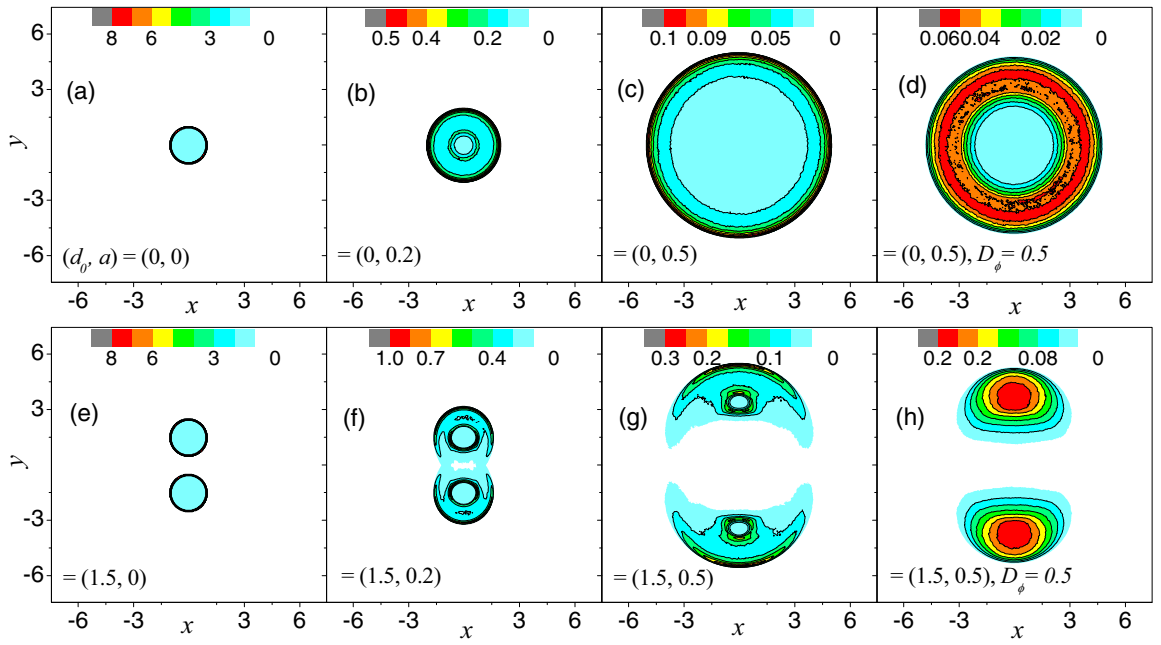

FIG. 2. Contour plots of $P_i(x,y)$ for the harmonically trapped active JP 1 (upper panels) and JP 2 (lower panels) at zero shear, $\Omega = 0$. The JPs' radius, a, and the centers of the JP 1 and 2 traps, $(0, \pm y_0)$, are reported in the legends; for $y_0 = 0$, (a)–(c), the contours of $P_i(x,y)$ coincide, for $y_0 > 0$, (e)–(g), are center-symmetric. Other simulation parameters are: $L = 50$, $h = 1$, $v_0 = 1$, $k = 1$, and $D_\phi = 0.05$. The simulation parameters in (d) and (h) are the same as, respectively, in (c) and (g), except for $D_\phi = 0.5$.

p.d.f.'s develop symmetric elliptic sub-structures [panel (f)]. The thickening of the p.d.f. ring-like sub-structure grows prominent with raising D_ϕ, as shown in panels (d) and (h); (iii) Most remarkably, on further increasing a above a certain critical value, a_c (which depends on y_0), the contours expand fast. For $y_0 = 0$, the $P_i(x,y)$ retain their ring-like structure, but their diameter, $r_\infty(a)$, increases exponentially with the hydrodynamical coupling [panel (c)], not much sensitive to D_ϕ [panel (d)]. For $y_0 > 0$, they peak a distance apart comparable to $r_\infty(a)$, with maxima centered on the y axis [panels (f) and (h)].

These properties are a consequence of the hydrodynamic pair coupling encoded in Eq. (1). More quantitatively, in Fig. 3(a) we plotted the average pair distance, $\langle r \rangle$, as a function of a for different trap distances and angular noise strengths. All curves develop a fast raising branch weakly dependent on y_0, for large a, whereas, in the opposite limit, the pair distance is much less sensitive to a, while growing linearly with y_0. For trap distances larger than the orbit diameter of the uncoupled JP's, $y_0 > v_0/k$, the transition between the regimes of weak interaction and mutual repulsion is quite abrupt, which defines a crossover coupling, a_c at constant film thickness, as a function of the trap distance. Increasing the intensity of the angular noise has the effect of lowering the active pair distance in both regimes.

On inspecting the contour plots of Figs. 2(c) and 2(g) one arrives at the conclusion that $\langle r \rangle$ at large a is comparable to the diameter, $r_\infty(a)$, of the $P_i(x,y)$ ring-like structure in panel (c) and the distance between their peaks in panel (g). This property signals a phase synchronization of the trapped particles. This hypothesis is corroborated in Fig. 3(b) by the a-dependence the ratio $R_\theta = -\langle \sin\theta_1 \sin\theta_2 \rangle / \langle \sin^2\theta_2 \rangle$, where θ_i are the particles' polar angles measured with respect to $\mathbf{d}_0$. For $a/h \to 0$, the two active JP's, which diffuse in circularly symmetric traps, are statistically uncorrelated and, therefore, the numerator of R_θ is identically zero. For $a > a_c$, due to the hydrodynamic repulsion, they tend to occupy positions diametrically opposite to the origin, that is, $\theta_1 = -\theta_2$, hence $R_\theta \to 1$. Moreover, the cross-over between the two opposite hydrodynamic interaction regimes in panels (a) and (b) of Fig. 3 are related, which confirms that the fast growth of $\langle r \rangle$ with a and the strong pair phase synchronization are manifestations of the same mechanism.

The dynamical transition occurring around $a \sim a_c$ is well illustrated by the equations for $\mathbf{r} = \mathbf{R}_1 - \mathbf{R}_2$, one easily derives from Eq. (1). By making use of the relevant polar coordinates r and θ, one obtains

$$
\begin{aligned}
r\frac{dr}{dt} &= \mathbf{r} \cdot [\lambda^r_- \Delta\mathbf{F} + \Delta\mathbf{u} + \Delta\mathbf{v}_0], \\
r^2\frac{d\boldsymbol{\theta}}{dt} &= \mathbf{r} \times [\lambda^\theta_- \Delta\mathbf{F} + \Delta\mathbf{u} + \Delta\mathbf{v}_0],
\end{aligned}
\tag{4}
$$

where $\Delta\mathbf{F} = \mathbf{F}_1 - \mathbf{F}_2$, $\Delta\mathbf{u} = \mathbf{u}_1 - \mathbf{u}_2$, $\Delta\mathbf{v}_0 = \mathbf{v}_{0,1} - \mathbf{v}_{0,2}$, and $\boldsymbol{\theta}$ is oriented in the $\hat{\mathbf{z}}$ direction (i.e., orthogonally to the film like in Fig. 1). The factors $\lambda^r_- = 1 - (a/h)\ln(L/r)$ and $\lambda^\theta_- = 1 - (a/h)[\ln(L/r) - 1]$ are the eigenvalues of the mobility tensor, $\mathbf{1}\delta^{\alpha\beta} + \mathbf{G}^{\alpha\beta}$, introduced in Eq. (1); they represent opposite particle displacements of coordinate r and θ, respectively [13].

The average pair distance as a function of a, $\langle r(a) \rangle$, is obtained by setting the time average of the r.h.s. of the first Eq. (4) to zero, that is, in the absence of shear, $\langle \mathbf{r} \cdot (\lambda^r_- \Delta\mathbf{F} + \Delta\mathbf{v}_0) \rangle = 0$. This returns two solutions. The first holds for weak hydrodynamic couplings, $a/h \to 0$, when $\lambda^r_- = \lambda^\theta_- \simeq 1$. As the orientations, ϕ_i, of the self-propulsion velocities, $\mathbf{v}_{0,i}$, freely fluctuate with time, in this regime both $\mathbf{F}_i(\mathbf{R}_i) + \mathbf{v}_{0,i}$ must vanish separately. The locus of $\mathbf{R}_i$ satisfying such a condition is a circle of radius v_0/k and center $\mathbf{d}_i$

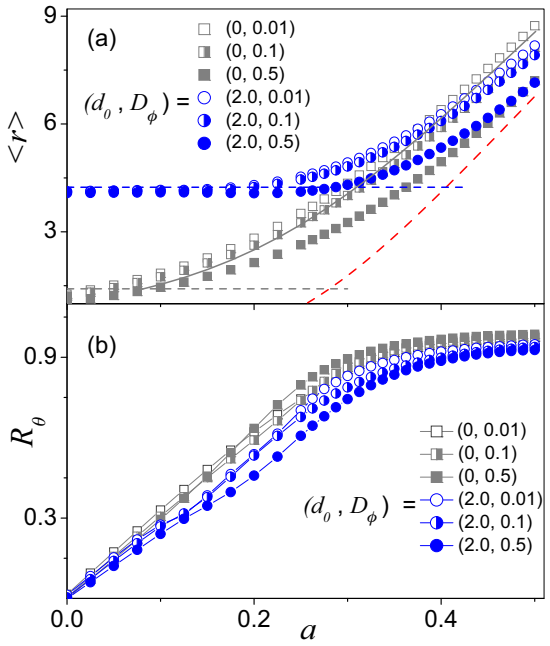

FIG. 3. Active JP's in harmonic traps with $\pm\mathbf{d}_0 = (0, \pm y_0)$, zero shear, $\Omega = 0$, and different D_ϕ: (a) average pair distance $\langle r\rangle$ vs. a; (b) angular synchronization factor R_θ vs. a (see text). Other simulation parameters are: $L = 50$, $h = 1$, $v_0 = 1$, and $k = 1$. The horizontal dashed curves in (a) represent our predictions for $\langle r\rangle$ at low a, r_0. Our estimates of $\langle r\rangle$ for $y_0 = 0$ and large a in the regime of high, $\bar{r}_\infty(a)$, and low angular noise, $r_\infty(a)$, are plotted, respectively, as dashed and solid curves. For a given y_0, r_0 and $\bar{r}_\infty(a)$ cross at the critical coupling, a_c.

[Figs. 2(a), 2(b)]. Correspondingly, the average pair distance for zero hydrodynamic coupling (no synchronization) and vanishingly low noise (no fluctuations of the pair center of mass) is $r_0 \equiv \langle r(0)\rangle = \sqrt{(2d_0)^2 + 2(v_0/k)^2}$. The effect of the hydrodynamic coupling in leading order of a/h follows a simple perturbation scheme, namely, $r_0 \to r_0 + (2/r_0)(a/h)(v_0/k)^2 \ln(L/r_0)$. As anticipated in the discussion of Fig. 3(a), the first order correction in a/h is strongly suppressed with increasing d_0. Finally, we notice that the angular noise tends to reduce the average radius of the particles' orbits [31].

The second solution for $\langle r\rangle$ can be derived in the limit $a \to h/2$ under the additional condition that the angular velocity $d\theta/dt$ in Eq. (4) vanishes. For short persistence times, that is relatively large D_ϕ/k ratios, the time average $\langle \mathbf{r}\cdot\Delta\mathbf{v}_0\rangle$ can be safely approximated to zero, so that the r.h.s. of the first Eq. (4) vanishes in correspondence with the zero of $\lambda^r_-(r) = 0$, whence $\langle r\rangle \simeq \bar{r}_\infty(a) = Le^{-h/a}$. This is an asymptotic solution that holds for large D_ϕ values, irrespective of the traps' distance d_0.

Under these conditions, for $d_0 = 0$ the r.h.s. of the second Eq. (4) vanishes when the two particles uniformly populate a circle. However, on discussing Fig. 2(c) we remarked that the average radius of such circle comes close to the average pair distance; this is only possible if the JP pair is synchronized with opposite phases, $\theta_1 = -\theta_2 = \theta$ (i.e., the fluctuations of the pair's center of mass are strongly suppressed). On the contrary, for $d_0 > 0$, the condition $d\theta/dt$ requires that in average $\mathbf{r}||\mathbf{d}_0$: therefore, the two JP's are still trapped on the circle of radius $r_\infty \simeq \bar{r}_\infty$, but fluctuate around the opposite extremities of the diameter parallel to $\mathbf{d}_0$, consistently with the numerical data plotted in Figs. 2(c) and 2(g). We stress once again that in suitably thin films both r_0 and $\bar{r}_\infty$ are much larger than a, so that pair collisions can be safely ignored.

For long persistence times, $D_\phi/k \to 0$, each particle approaches a position of quasi-equilibrium inside its own trap, which depends on the orientation of $\mathbf{v}_{0i}$ and varies adiabatically with time. When the active pair sits in the same trap, $d_0 = 0$, the ensuing stationary condition yields the transcendental equation

$$\lambda^r_-(\langle r\rangle) = \frac{v_0}{k\langle r\rangle}, \tag{5}$$

whose numerical solution, $\langle r\rangle = r_\infty(a)$, is drawn in Fig. 3(a). Here we made use of the pair's centersymmetric configuration to approximate $\langle \mathbf{r}\cdot\Delta\mathbf{v}_0\rangle$. An analytical estimate of the low-noise dependence of $\langle r\rangle$ on d_0 is a more complicated task and will not be pursued here.

Our predictions for r_0 and r_∞ are illustrated in Fig. 3(a). Note that $r_\infty(a)$ is strictly larger than $\bar{r}_\infty(a)$, which implies the stability of the first Eq. (4). The transition between the regimes of weak and strong hydrodynamic coupling occurs around a critical value, a_c, which increases with d_0. A simple geometric estimate of a_c is shown in Fig. 3(a) as the intersection of $\bar{r}_\infty(a)$ with r_0.

IV. COUETTE FLOW, Ω > 0

In the presence of a linear shear flow the dynamics of the trapped pair undergoes two remarkable changes: (1) Both particles are subjected to a shear torque, say, with $\Omega > 0$. As a consequence, they move counterclockwise along closed elliptical orbits, which are only slightly perturbed by noise as long as $D_\phi \ll \Omega$ (*chiral* dynamics [30,31]); (2) The Couette flow is characterized by a stream direction (here, parallel to the x axis) and a shear gradient orthogonal to it. This causes a dynamical symmetry breaking depending on whether the trap separation is parallel to $\hat{\mathbf{x}}$ or $\hat{\mathbf{y}}$. In Fig. 4 the contour plots of the particles' p.d.f.'s are displayed for $d_0 = 0$ (same trap, top row panels) and $\mathbf{d}_0 = (\pm x_0, 0)$ (trap shifted in the $\hat{\mathbf{x}}$ direction, bottom row panels). The transition between a regime of low hydrodynamic coupling, mostly governed by the chiral dynamics of a single active JP in a sheared harmonic trap [31] [panels (a), (e)], and a regime of strong coupling, dominated by an effective hydrodynamic repulsion [panels (c), (g)], is apparent. The overall top-left to bottom-right twisting of the contours is mostly a shearing effect [31].

The axis lengths of the elliptical structures of the 2D $P_i(x, y)$ in panels (a) and (e) are of the order of v_0/k, whereas the distance between their maxima in panels (c) and (g) (i.e., at large a) grows exponentially with a/h, like in Fig. 3(a). This behavior persists even in the presence of stronger angular noise, see panels (d) and (h). Quantitative measurements of the pair distance $\langle r\rangle$ are reported in Fig. 5 for $\mathbf{d}_0$ parallel to either $\hat{\mathbf{x}}$ or $\hat{\mathbf{y}}$. At low a, $\langle r\rangle$ is the same as for $\Omega = 0$ [Fig. 3(a)], independent of the $\mathbf{d}_0$ orientation. On the contrary, for $a \gg a_c$ and $d_0 > v_0/k$, the pair distance tends to grow larger (smaller) when $\mathbf{d}_0$ is orthogonal (parallel) to the flow; this suggests a

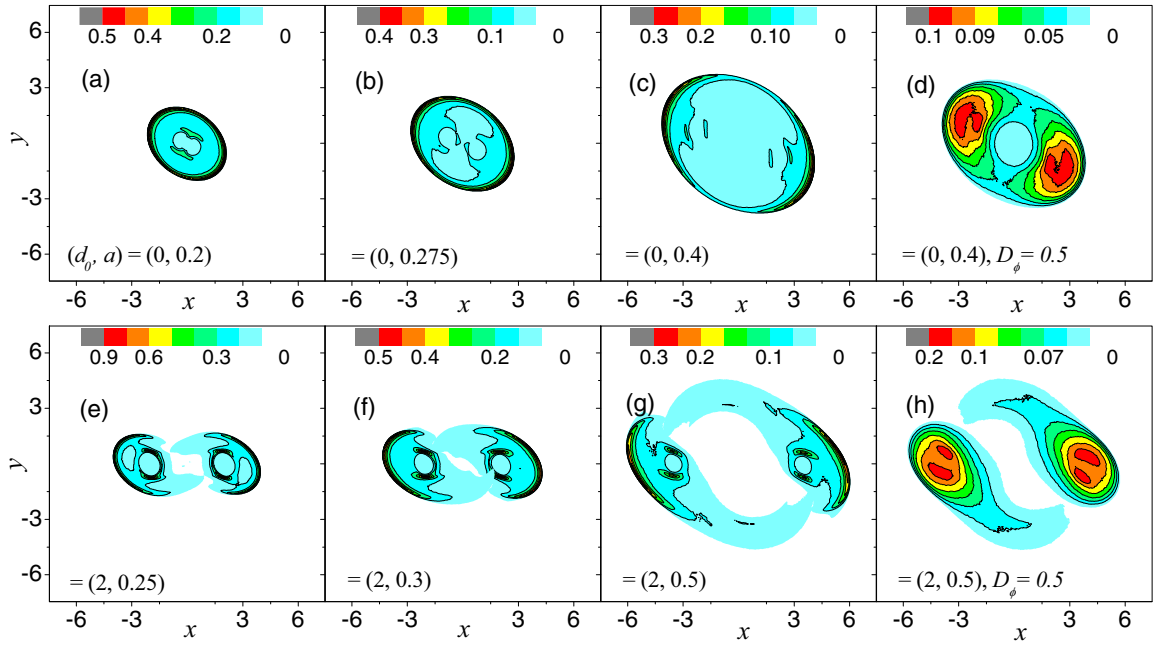

FIG. 4. Contour plots of $P_i(x, y)$ for two identical harmonically trapped active particles, JP 1 (right) and JP 2 (left), in a Couette shear flow with $\Omega = 0.1$. The particles' radius, a, and the traps' centers, $(\pm x_0, 0)$, vary as in the legends. Other simulation parameters are: $L = 50$, $h = 1$, $v_0 = 1$, $k = 1$, and $D_\phi = 0.05$. The simulation parameters in (d) and (h) are the same as, respectively, in (c) and (g), except for $D_\phi = 0.5$.

stronger (weaker) effective pair repulsion. Further numerical data (not reported) show that the dependence of $r_\infty(a)$ on the shear torque, Ω, is relatively small.

More intriguing is the pair dynamics at the transition, $a \sim a_c$ [Figs. 4(b), 4(f)]. Inside the same trap, $d_0 = 0$, the orbits of the two active JP's tend to disentangle due to repulsion, through a sort of spontaneous breaking of the pair symmetry. Of course, the relevant p.d.f.'s are identical, but two distinct peaks emerge as a result [panels (b), (c)]. In separated traps, $d_0 > 0$, the transition mechanism differs for $\mathbf{d}_0$ parallel to $\hat{\mathbf{x}}$ or $\hat{\mathbf{y}}$. Such an effect is apparent in Fig. 5(a) for trap distances of the order of or larger than the orbit size, i.e., for $d_0 > v_0/k$. This is a combined effect of shear torque and hydrodynamic coupling. The fluid velocity field, $\mathbf{u}_s(y)$, tends to pull the JPs' apart in the $\hat{\mathbf{x}}$ direction, thus causing an additional increase of the effective distance between the trapped particles. Accordingly, due to the shear flow, in Fig. 5(b) the synchronization factor, R_θ, vanishes for $a/h \to 0$ when $\mathbf{d}_0 || \hat{\mathbf{x}}$, but not when $\mathbf{d}_0 || \hat{\mathbf{y}}$.

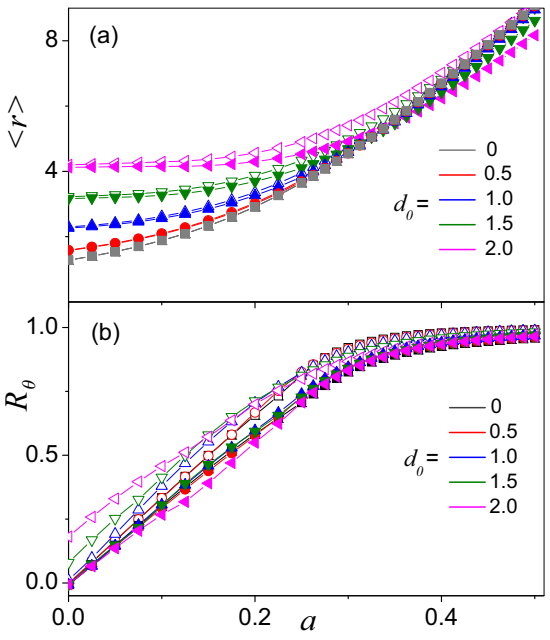

FIG. 5. Harmonically trapped active JP's in a Couette shear with $\Omega = 0.1$: $\langle r \rangle$ (a) and R_θ (b) vs. a for $\mathbf{d}_0 || \hat{\mathbf{x}}$ (filled symbols) and $\mathbf{d}_0 || \hat{\mathbf{y}}$ (empty symbols). Other simulation parameters are: $L = 50$, $h = 1$, $v_0 = 1$, $k = 1$, and $D_\phi = 0.01$.

Finally, another interesting property of the active JP pair dynamics in the transition regime was observed in the noiseless limit, $D_\phi \equiv 0$, namely the appearance of chaotic trajectories driven by the shear torque. Samples of the two JPs' trajectories for different model parameters are displayed in Fig. 6.

V. CONCLUSIONS

In conclusion, we have investigated how hydrodynamic coupling affects the 2D dynamics of a pair of active microswimmers self-propelling in a thin viscous film. As one drives them closer and closer by means of two harmonic traps, say, two optical tweezers, they eventually repel one another to the point that their final average distance is determined by the hydrodynamic coupling rather than by the traps' separation. In this experimental scheme, encoded in our model equations, each active JP is harmonically bound to its own trap. This makes sense as long as the effective truncated trap's radius is larger than the radius of the particle's orbit in the trap, but smaller than the resulting average pair distance. Based on our numerical simulations, the predicted pair

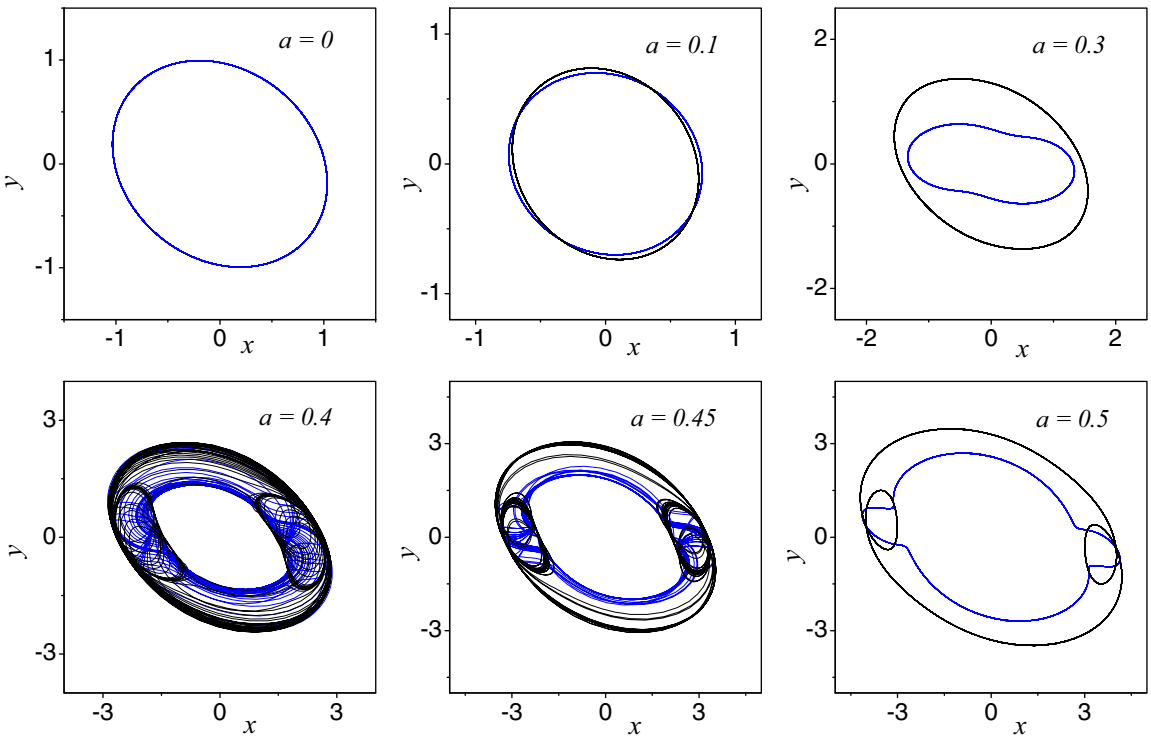

FIG. 6. Trajectories of two active JP's bound to the same harmonic trap centered at the origin, $d_0 = 0$, in the absence of angular noise, $D_\phi = 0$, and subjected to a Couette shear with $\Omega = 0.1$. The initial conditions are the same in all panels, $x_1(0) = 0$, $y_1(0) = 0$, $\phi_1(0) = 0$, and $x_2(0) = 1$, $y_2(0) = 0$, $\phi_2(0) = 0.045\pi$. whereas a has been varied as reported in the legends. Other simulation parameters are: $L = 50$, $v_0 = 1$, and $k = 1$; the trajectories of JP1 and JP2 are drawn, respectively, in blue and black.

synchronization turns out to be more persistent than reported for both passive [32] and active [33] colloidal particles in a 3D trap.

Our analysis was carried out under two simplifying assumptions: (1) The active JP pair was freely moving inside a thin free-standing film [13], far away from any geometric obstacle. Diffusion perpendicular to the film was then neglected as the film thickness was taken small compared to the JP orbit size for any value of the hydrodynamic coupling; (2) The traps were modeled as isotropic and harmonic. In a real optical tweezer the confining force is linear only close to the center, while additional effects due to the radiation pressure may arise in the outer regions. For relatively weak particle activation, such nonlinear contributions can be safely neglected [23].

ACKNOWLEDGMENTS

We thank RIKEN, Japan, for granting access to their Hokusai supercomputer. Y.L. is supported by the NSF China under grant no. 11505128. P.K.G. was supported by a SERB Start-up Research Grant (Young Scientist) No. YSS/2014/000853 and the UGC-BSR Start-Up Grant No. F. 30-92/2015. T.D. thanks UGC, New Delhi, India, for support through a Junior Research Fellowship.

T.D. and Y.L. equally contributed as first authors.

[1] *Janus Particle Synthesis, Self-Assembly and Applications*, edited by S. Jiang and S. Granick (RSC Publishing, Cambridge, 2012).

[2] A. Walther and A. H. E. Müller, Janus particles: Synthesis, self-assembly, physical properties, and applications, Chem. Rev. **113**, 5194 (2013).

[3] J. Elgeti, R. G. Winkler, and G. Gompper, Physics of microswimmers, single particle motion and collective behavior: A review, Rep. Progr. Phys. **78**, 056601 (2015).

[4] R. Golestanian, T. B. Liverpool, and A. Adjari, Designing phoretic micro- and nano-swimmers, New J. Phys. **9**, 126 (2007).

[5] W. E. Uspal, H. Burak Eral, and P. S. Doyle, Engineering particle trajectories in microfluidic flows using particle shape, Nat. Commun. **4**, 2666 (2013).

[6] S. Das, A. Garg, A. I. Campbell, J. Howse, A. Sen, D. Valegol, R. Golestanian, and S. J. Ebbens, Boundaries can steer active Janus spheres, Nat. Commun. **6**, 8999 (2015).

[7] A. Zöttl and H. Stark, Emergent behavior in active colloids, J. Phys.: Condens. Matter **28**, 253001 (2016).

[8] J. Palacci, S. Sacanna, A. Abramian, J. Barral, K. Hanson, A. Y. Grosberg, D. J. Pine, and P. M. Chaikin, Artificial rheotaxis, Sci. Adv. **1**, e1400214 (2015).

[9] E. Lauga and T. R. Powers, The hydrodynamics of swimming microorganisms, Rep. Prog. Phys. **72**, 096601 (2009).

[10] M. C. Marchetti, J. F. Joanny, S. Ramaswamy, T. B. Liverpool, J. Prost, and Madan Rao, Hydrodynamics of soft active matter, Rev. Mod. Phys. **85**, 1143 (2013).

[11] C. Cheung, Y. H. Hwang, X.-I. Wu, and H. J. Choi, Diffusion of Particles in Free Standing Liquid Films, Phys. Rev. Lett. **76**, 2531 (1996).

[12] B. Cui, H. Diamant, B. Lin, and S. A. Rice, Anomalous Hydrodynamic Interaction in a Quasi-Two-Dimensional Suspension, Phys. Rev. Lett. **92**, 258301 (2004).

[13] R. Di Leonardo, S. Keen, F. Ianni, J. Leach, M. J. Padgett, and G. Ruocco, Hydrodynamic interactions in two dimensions, Phys. Rev. E **78**, 031406 (2008).

[14] S. Sengupta, M. E. Ibele, and A. Sen, Fantastic voyage: Designing self-powered nanorobots, Angew. Chem. Int. Ed. **51**, 8434 (2012).

[15] T. Tlusty, Screening by symmetry of long-range hydrodynamic interactions of polymers confined in sheets, Macromolecules **39**, 3927 (2006).

[16] D. Takagi, A. B. Braunschweig, J. Zhang, and M. J. Shelley, Dispersion of Self-Propelled Rods Undergoing Fluctuation-Driven Flips, Phys. Rev. Lett. **110**, 038301 (2013).

[17] A. Ziehl, J. Bammert, L. Holzer, C. Wagner, and W. Zimmermann, Direct Measurements of Shear-Induced Cross-Correlations of Brownian Motion, Phys. Rev. Lett. **103**, 230602 (2009).

[18] J. Bammert, L. Holzer, and W. Zimmermann, Dynamics of two trapped Brownian particles: Shear-induced cross-correlations, Eur. Phys. J. E **33**, 313 (2010).

[19] J.-C. Meiners and S. R. Quake, Direct Measurement of Hydrodynamic Cross Correlations Between Two Particles in an External Potential, Phys. Rev. Lett. **82**, 2211 (1999).

[20] X. Yang, C. Liu, Y. Li, F. Marchesoni, P. Hänggi, and H. P. Zhang, Hydrodynamic and entropic effects on colloidal diffusion in corrugated channels, Proc. Natl. Acad. Sci. USA **114**, 9564 (2017).

[21] C. Pozrikidis, *Fluid Dynamics*, 2nd ed. (Springer, New York, 2009).

[22] T. Debnath, P. K. Ghosh, F. Nori, Y. Li, F. Marchesoni, and B. Li, Diffusion of active dimers in a Couette flow, Soft Matter **13**, 2793 (2017).

[23] H. W. Moyses, R. O. Bauer, A. Y. Grosberg, and D. G. Grier, A perturbative theory for Brownian vortexes, Phys. Rev. E **91**, 062144 (2015).

[24] R. Golestanian, T. B. Liverpool, and A. Adjari, Self-Motile Colloidal Particles: From Directed Propulsion to Random Walk, Phys. Rev. Lett. **99**, 048102 (2007).

[25] D. Debnath, P. K. Ghosh, Y. Li, F. Marchesoni, and B. Li, Diffusion of eccentric microswimmers, Soft Matter **12**, 2017 (2016).

[26] A. Zöttl and H. Stark, Nonlinear Dynamics of a Microswimmer in Poiseuille Flow, Phys. Rev. Lett. **108**, 218104 (2012).

[27] T. Bickel, G. Zecua, and A. Würger, Polarization of active Janus particles, Phys. Rev. E **89**, 050303 (2014).

[28] B. ten Hagen, R. Wittkowski, D. Takagi, F. Kümmel, C. Bechinger, and H. Löwen, Can the self-propulsion of anisotropic microswimmers be described by using forces and torques? J. Phys.: Condens. Matter **27**, 194110 (2015).

[29] By means of a standard Mil'shtein algorithm, see P. E. Kloeden and E. Platen, *Numerical Solution of Stochastic Differential Equations* (Springer, Berlin, 1992).

[30] S. van Teeffelen and H. Löwen, Dynamics of a Brownian circle swimmer, Phys. Rev. E **78**, 020101 (2008).

[31] Y. Li, F. Marchesoni, T. Debnath, and P. K. Ghosh, Dynamics of a trapped active swimmer in a shear flow, Phys. Rev. E **96**, 062138 (2017).

[32] J. Kotar, M. Leoni, B. Bassetti, M. Cosentino Lagomarsino, and P. Cicuta, Hydrodynamic synchronization of colloidal oscillators, Proc. Natl. Acad. Sci. USA **107**, 7669 (2010).

[33] R. Matas Navarro and I. Pagonabarraga, Hydrodynamic interaction between two trapped swimming model micro-organisms, Eur. Phys. J. E **33**, 27 (2010).